

Take an Emotion Walk: Perceiving Emotions from Gaits Using Hierarchical Attention Pooling and Affective Mapping

Uttaran Bhattacharya, Christian Roncal, Trisha Mittal, Rohan Chandra,
Aniket Bera, Dinesh Manocha

Department of Computer Science, University of Maryland, College Park, USA
<http://www.gamma.umd.edu/taew>

Abstract

We present an autoencoder-based semi-supervised approach to classify perceived human emotions from walking styles obtained from videos or from motion-captured data and represented as sequences of 3D poses. Given the motion on each joint in the pose at each time step extracted from 3D pose sequences, we hierarchically pool these joint motions in a bottom-up manner in the encoder, following the kinematic chains in the human body. We also constrain the latent embeddings of the encoder to contain the space of psychologically-motivated affective features underlying the gaits. We train the decoder to reconstruct the motions per joint per time step in a top-down manner from the latent embeddings. For the annotated data, we also train a classifier to map the latent embeddings to emotion labels. Our semi-supervised approach achieves a mean average precision of 0.84 on the Emotion-Gait benchmark dataset, which contains gaits collected from multiple sources. We outperform current state-of-art algorithms for both emotion recognition and action recognition from 3D gaits by 7% – 23% on the absolute.

1. Introduction

Humans perceive each other's emotions and moods through verbal cues such as speech [47, 27] and text [56, 12], as well as through non-verbal cues or *affective features* [48], including eye-movements [50], facial expressions [18], tone of voice, postures [4], and walking styles [32]. Understanding these perceived emotions shapes people's interactions and experiences, especially when performing tasks in collaborative or competitive environments [6]. Given the importance of perceived emotions in everyday lives, there has consequently been a keen interest in developing automated techniques for perceiving human emotions from various cues, with applications in affective computing, therapy, and rehabilitation [49], robotics [7],

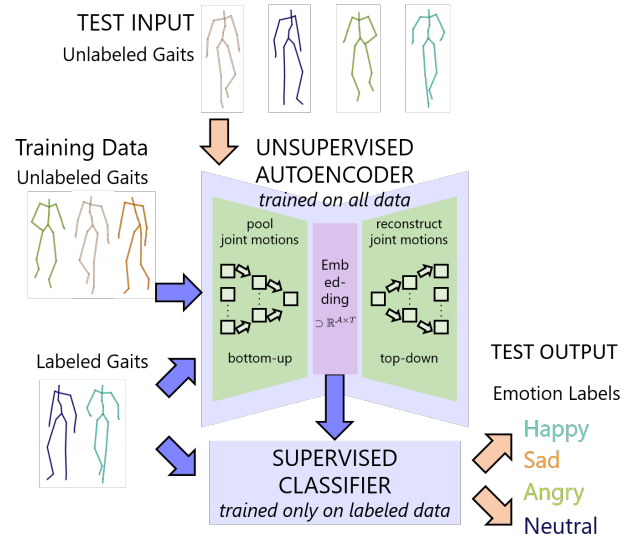


Figure 1. **Perceiving Emotions from Gaits.** We present a semi-supervised approach to predict discrete perceived emotions from 3D pose sequences of human gaits. Our unsupervised autoencoder learns latent embeddings for all the labeled and unlabeled input gaits using hierarchical pooling. Our supervised classifier learns to predict emotion labels by training only the labeled gaits. The autoencoder and the classifier are trained together to accurately classify the unlabeled data. Our overall approach can utilize a large number of unlabeled gaits to improve accuracy. In practice, the mean average precision of our network increases linearly with the size of the unlabeled training data.

surveillance [3], audience understanding [59], character generation [55] and many more areas.

While there are multiple non-verbal modalities for perceiving emotions, in our work, we limit ourselves to the affective features expressed through peoples' styles of walking or their "gaits", extracted from videos or from motion-captured data, as a cue for perceiving emotions. Perceived emotion recognition using any form of affective features is

considered to be a challenging problem in both psychology and AI, primarily because of the unreliability in both the cues and the perception from the cues. Unreliability can arise from a variety of sources, such as “mock” expressions [17], expressions affected by the presence or absence of an audience [19], or even self-reported emotions when subjects anticipate negative repercussions [43]. In our work, we only consider the emotions of subjects as perceived from their gaits by observers and not self-reported emotions. Studies in psychology have shown that observers were able to perceive the emotional states of walking subjects by observing features such as arm swinging, stride lengths, collapsed upper body, etc. [39, 32]. These features hold useful information for perceiving emotions and are collectively known as affective features expressed from gaits.

Gaits and 3D poses have been widely used in computer vision for many applications, including action recognition and perceiving emotions [62, 52]. However, there are a few key challenges in terms of designing machine learning methods for emotion recognition using gaits:

- Many prior techniques designed for predicting perceived emotions from gaits use the biomechanical features extracted from human gaits, but these methods suffer from low prediction accuracy [15, 57].
- More recent methods have trained supervised networks to achieve high emotion prediction accuracy [46, 9], but these methods heavily rely on sufficiently large sets of annotated data. Annotations are expensive and tedious, due to the variations in scales and motion trajectories [2], as well as the inherent subjectivity in perceiving emotions [9]. The state of the datasets for emotion recognition, Emotion-Gait [9], has around 4,000 data points of which more than 53% are unlabeled.
- Generating class-conditioned data from gaits is a popular approach to augment datasets, but current methods can only generate data for short time periods [24, 30] or with relatively low diversity [45, 61, 63, 9].

On the other hand, recent advances in gait extraction and 3D pose computation are making it possible to automatically extract unlabeled gaits from videos and they can be used to learn meaningful representations for various tasks [24, 45]. Thus, given the availability of large (unlabeled) gait datasets and the sparsity of (labeled) gaits with perceived emotions, there is a need to develop automatic methods that can combine these datasets for emotion recognition.

Main Contributions: We present a semi-supervised network that takes in 3D pose sequences of human gaits, extracted either from videos or from motion-captured data, and predicts discrete perceived emotions, such as happy, angry, sad and neutral. Our network consists of an unsupervised autoencoder coupled with a supervised classifier.

The encoder in the unsupervised autoencoder hierarchi-

cally pools attentions on parts of the body, *i.e.*, it learns separate intermediate feature representations for the motions on each of the human body parts (arms, legs, and torso) and then pools these features in a bottom-up manner to map them to the latent embeddings of the autoencoder. The decoder takes in these embeddings and reconstructs the motion on each joint of the body in a top-down manner.

We also perform affective mapping, *i.e.*, we constrain the embeddings to contain the space of psychologically-motivated affective features expressed from the input gaits since these features contain useful information for distinguishing between different perceived emotions.

Lastly, for the labeled data, our supervised classifier learns to map the embeddings from the encoder to the discrete emotion labels to complete the training process. The novel components of our work include:

- A semi-supervised network, consisting of an autoencoder and a classifier that are trained together, to predict discrete perceived emotions from 3D pose sequences of gaits of humans.
- A hierarchical attention pooling module on the autoencoder to learn useful embeddings for unlabeled gaits, which improves the mean average precision in classification by 1–17% on the absolute compared to state-of-the-art methods in both emotion recognition and action recognition from 3D gaits on the Emotion-Gait benchmark dataset.
- Constraining the network to map the learned embeddings to the psychologically-motivated affective features expressed from the input gaits to improve the overall network performance. This improves the mean average precision in classification by 7 – 23% on the absolute compared to state-of-the-art methods.
- The performance of our network improves linearly as more unlabeled data is used for training. More importantly, we report 10 – 50% improvement on average precision on the absolute for emotion classes that have fewer than 25% labeled samples in Emotion-Gait.

2. Related Work

In this section, we briefly review prior work in classifying perceived emotions from gaits, as well as the related task of action recognition and generation from gaits.

Classification of Perceived Emotions from Gaits. Gaits have been studied as a modality for recognizing perceived emotions in both psychology and AI. Experiments have shown that participants were able to identify sadness, anger, happiness, and pride by observing gait features such as arm swinging, long strides, erect posture, collapsed upper body, etc. [41, 36, 39, 32]. This, in turn, has led to considerable interest from both the computer vision and the affective computing communities in classifying perceived emotions from recorded gaits. Karg et al. [29] used

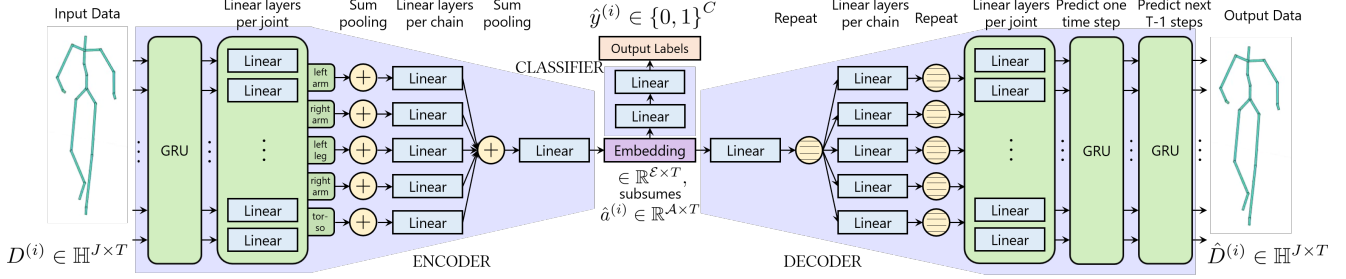


Figure 2. **Our network for semi-supervised classification of discrete perceived emotions from gaits.** Inputs to the encoder are rotations on each joint at each time step, represented as 4D unit quaternions. The inputs are pooled bottom-up according to the kinematic chains of the human body. The embeddings at the end of the encoder are constrained to lie in the space of the mean affective features \mathbb{R}^A . For labeled data, the embeddings are passed through the classifier to predict output labels. The linear layers in the decoder take in the embeddings and reconstruct the motion on each joint at a single time-step at the output of the first GRU. The second GRU in the decoder takes in the reconstructed joint motions at a single time step and predicts the joint motions for the next $T - 1$ time steps.

PCA-based classifiers, and Crenn et al. [15] used SVMs on psychologically-motivated affective features. Venture et al. [57] used autocorrelation matrices between joint angles to perform similarity-based classification. Daoudi et al. [16], on the other hand, performed nearest neighbor classification on symmetric positive definite matrices crafted from joint movements. More recently, Randhavane et al. [46] combined features learned from an LSTM-based network with affective features to classify gaits into one of four perceived emotion classes. Bhattacharya et al. [9] combined affective features with features obtained from a graph convolution-based network to perform a similar classification.

Action Recognition and Generation. Modeling of human gaits has been extensively studied in both computer vision and computer graphics, primarily in the context of supervised action recognition [13, 60] and unsupervised action generation [63, 61]. Prior works have developed sophisticated networks for action recognition and generation by exploiting 2D pose sequences extracted from videos [13, 60, 63, 30], as well as 3D pose sequences obtained from motion-captured data [62, 24, 45].

Since 2D and 3D poses can be naturally modeled as graphs, gaits, by extension, can be naturally modeled as graph sequences. Therefore, both graph convolution-based approaches [62] and RNN-based approaches [66] have been successful in performing action recognition from gaits [62]. Recently, Si et al. [54] applied graph convolutions inside LSTM gates to improve recognition accuracies for actions such as walking, running, etc. on benchmark datasets such as Human3.6M [26]. Shi et al. [52] trained a network with directed graphs modeled on kinematic dependencies between joints and bones, and Shi et al. [53] combined two separate networks, one trained with poses and the other trained with second-order derivatives of poses. Both showed significant improvements in action recogni-

tion tasks on the NTU RGB+D [51] and Kinetics [11] datasets. Wang et al. [58] provide a comprehensive review of all the recent Kinect-based action recognition methods.

RNN and convolution-based approaches have also been extended to semi-supervised classification. Harvey et al. [22] have employed a per-frame reconstruction and classification loss to train an RNN-based semi-supervised network on MOCAP datasets. Pavllo et al. [44] used a series of convolutional layers on 3D pose sequences and constrained the limb dimensions to transform the input into a latent representation for both classification and generation. Kanazawa et al. [28] and Zhang et al. [65] respectively developed semi-supervised networks and unsupervised autoregressive networks, which encode temporal data to predict short-term human dynamics from a small set of labeled videos and a large set of scraped, unlabeled videos.

Generative methods have also exploited sequences of 2D or 3D human poses to train neural networks. For example, in [64, 10], the initial poses, and the intermediate transformations between frames are learned through separate networks and combined into a unified network that generates gaits. Other approaches model generation as a sequence prediction problem subject to constraints such as position and movement constraints on various limbs [2], action-specific trajectory constraints [24], and structural and kinematic constraints of the human joints [45].

In our work, we learn latent embeddings from gaits by exploring the kinematic chains in the human body [5]. These chains contain useful motion constraints, which, to the best of our knowledge, has not been explored in methods using 3D pose-based gaits. Inspired by prior works in emotion perception from gaits, we also constrain our embeddings to contain the space of affective features expressed from gaits, to improve our classification performance.

3. Approach

Our goal is to classify input 3D pose sequences of human gaits, recorded using motion capture or extracted from videos to one or more discrete perceived emotion labels such as happy, sad, angry, etc. We first provide a brief background on representing discrete emotions in Section 3.1. We then discuss our preprocessing step for representing labeled and unlabeled datasets in Section 3.2.

Given both labeled and unlabeled data, we use a semi-supervised approach to classify all the data. Figure 2 shows our overall network for semi-supervised learning. Our architecture is composed of an autoencoder coupled with a classifier. Given 3D pose sequences, we first extract the rotation per joint, as described in Section 3.2, from the first frame to the current frame. We then pass these rotations through our encoder network represented by $f_\theta(\cdot)$, where θ is the set of trainable weights and biases in the encoder. The encoder transforms the input rotations into a feature representation in the latent embedding space. Next, we pass the feature through a decoder network, similarly represented by $f_\psi(\cdot)$, to generate reconstructions of the input rotations, which are used to learn the embedding space. Additionally, if training labels are available, we also pass the encoded feature representations through a simple fully-connected classifier network, represented by $f_\phi(\cdot)$, to predict the probabilities of the discrete labels. We define the loss function of the entire network as:

$$\mathcal{C}(\theta, \phi, \psi) = \sum_{i=1}^M I_y^{(i)} \mathcal{C}_{CL} \left(y^{(i)}, f_{\phi \circ \theta} \left(D^{(i)} \right) \right) + \mathcal{C}_{AE} \left(D^{(i)}, f_{\psi \circ \theta} \left(D^{(i)} \right) \right), \quad (1)$$

where $f_{b \circ a}(\cdot) := f_b(f_a(\cdot))$ denotes the composition of functions, $I_y^{(i)}$ is an indicator variable denoting whether the i^{th} data point has an associated label $y^{(i)}$, \mathcal{C}_{CL} denotes the classifier loss detailed in Section 3.3, and \mathcal{C}_{AE} denotes the autoencoder loss detailed in Section 3.4. For brevity of notation, we will henceforth use $\hat{y}^{(i)} := f_{\phi \circ \theta} \left(D^{(i)} \right)$ and $\hat{D}^{(i)} := f_{\psi \circ \theta} \left(D^{(i)} \right)$.

3.1. Representing Emotions

The Valence-Arousal-Dominance (VAD) model [38] is a well-known model for representing emotions in a continuous space. This model assumes three independent axes, representing valence, arousal, and dominance values, that collectively indicate an observed emotion. Valence indicates how pleasant the emotions are, arousal indicates how intensely the emotions are expressed, and dominance indicates how much an observer feels dominated when observing the emotions. For example, happiness is a pleasant emotion, therefore has a high valence, while anger and sadness

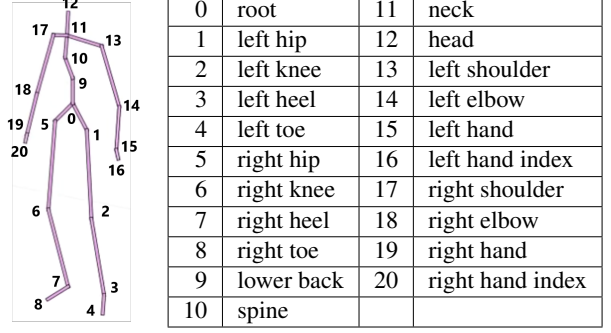


Figure 3. **3D pose model.** The names and numbering of the 21 joints in the pose follow the nomenclature in the ELMD dataset compiled by Habibie et al. [21].

Table 1. **Affective Features.** List of the 18 pose affective features that we use to describe the affective feature space for our network.

Angles between	shoulders at lower back
	hands at root
	left shoulder and hand at elbow
	right shoulder and hand at elbow
	head and left shoulder at neck
	head and right shoulder at neck
	head and left knee at root
	head and right knee at root
	left toe and right toe at root
	left hip and toe at knee
	right hip and toe at knee
Distance ratios between	left hand index (LHI) to neck and LHI to root
	right hand index (RHI) to neck and RHI to root
	LHI to RHI and neck to root
	left toe to right toe and neck to root
Area (Δ) ratios between	Δ shoulders to lower back and Δ shoulders to root
	Δ hands to lower back and Δ hands to root
	Δ hand indices to neck and Δ toes to root

are unpleasant and have low valence. Anger is often intensely expressed, so it has high arousal, while expressions of sadness are often reserved, leading it to have low valence. Anger or excitement can also make an observer feel dominated, and therefore has high dominance, while fear is often more submissive, and therefore has low dominance.

While the VAD model is well-understood in psychology, discrete emotion terms are more easily understood by non-expert annotators and end-users. Moreover, prior studies have shown that discrete emotions can be mapped back to the VAD space through various transforms [37, 23]. Therefore, most existing datasets for supervised emotion classification annotate data with discrete emotion labels, and most supervised methods report performance on predicting these discrete labels. In the interest of having consistent evaluation metrics to compare our approach with existing methods, we choose to use discrete emotion labels in our work as well.

3.2. Representing the Data

Given the 3D pose sequences for gaits, our first task is to obtain the rotations per joint per time step in the pose to feed into the network.

We denote a gait as $G = \{(x_j^t, y_j^t, z_j^t)\}_{j=1, t=1}^{J, T}$, which consists of the 3D positions of J joints across T time steps. We denote the rotation of joint j from the first frame to time step t as $R_j^t \in \mathbb{SO}(3)$. Following the approach taken by Pavllo et al. [45], we represent these rotations as unit quaternions $q_j^t \in \mathbb{H} \subset \mathbb{R}^4$, where \mathbb{H} denotes the space of unit 4D quaternions. We have chosen to represent rotations as quaternions as they are free of the gimbal-lock problem, unlike other common representations such as Euler angles or exponential maps [20]. We enforce the additional unit norm constraints for these quaternions when training our autoencoder. We represent the overall input to our network as $D^{(i)} := \{q_j^t\}_{j=1, t=1}^{J, T} \in \mathbb{H}^{J \times T}$.

3.3. Label Construction and Classifier Loss

Emotion perception is an inherently subjective task [32]. For example, a gait that appears happy to one observer can appear neutral or even angry to others. Predicting a gait to belong to only one emotion class can thus lead to misleading and even incorrect inferences [40]. We, therefore, use multi-hot labels to assign each gait to one or more classes. We now describe the process of constructing the multi-hot labels for our training process and how we use it to formulate the classifier loss function.

We assume that the given labeled gait dataset consists of C discrete emotion classes. The raw label vector $L^{(i)}$ for the i^{th} gait is a probability vector, where the l^{th} element of the vector denotes the probability that the corresponding gait appears to have the l^{th} emotion, *i.e.*, we assume $L^{(i)} \in [0, 1]^C$ to be given as

$$L^{(i)} = [p_1 \ p_2 \ \dots \ p_C]^\top \quad (2)$$

where p_l denotes the probability of the l^{th} emotion and $l = 1, 2, \dots, C$. In practice, the probability of each emotion for each labeled gait in a dataset is obtained as the fraction of annotators who labeled the gait with the corresponding emotion.

In order to perform classification, we need to convert each element in $L^{(i)}$ to an assignment in $\{0, 1\}$. Taking into account the subjectivity in perceived emotions, we consider a gait to belong to a class l whenever $p_l > \frac{1}{C}$, *i.e.*, the gait has more than a random chance of belonging to that class.

Thus, we represent the processed emotion labels as multi-hot vectors $y^{(i)} \in \{0, 1\}^C$, where we set the value for classes with probability more than $\frac{1}{C}$ in $L^{(i)}$ to be 1, and 0 otherwise.

Since our classification problem is multi-class (typically, $C > 2$) as well as multi-label (a gait can belong to one

or more classes), we use the weighted multi-class cross-entropy loss

$$\mathcal{C}_{CL} \left(y^{(i)}, \hat{y}^{(i)} \right) := - \sum_{l=1}^C w_l (y_l)^{(i)} \log (\hat{y}_l)^{(i)} \quad (3)$$

for our classifier loss, where $(y_l)^{(i)}$ and $(\hat{y}_l)^{(i)}$ denote the l^{th} components of $y^{(i)}$ and $\hat{y}^{(i)}$, respectively. We also add the fixed per-class weights $w_l = e^{-p_l}$ to make the training more sensitive to mistakes on the rarer samples in the annotated dataset.

3.4. Affective Features and Autoencoder Loss

Based on prior studies in psychology [15], a person’s perceived emotions can be accurately represented by a set of scale-independent affective pose features. We consider the pose to be made up of $J = 21$ joints as identified in Figure 3. Following Randhavane et al. [46], we categorize the affective pose features in the following 3 types:

- *Angles.* Consists of angles at different joints, such as between the head and the neck (used to compute head tilt), the neck, and the shoulders (used to compute slouching), root and thighs (used to compute stride lengths), etc.
- *Distance ratios.* Consists of distance ratios such as the ratio between the distance from the hand to the neck, and that from the hand to the root (used to compute arm swings).
- *Area ratios.* Consists of ratios of areas formed by a triplet of joints, such as the ratio of the area formed between the elbows and the neck and the area formed between the elbows and the root (used to compute slouching and arm swings).

We present the full list of the $\mathcal{A} = 18$ affective features we use in Table 1. We denote the set of affective pose features across all time steps for the i^{th} gait as $a^{(i)} \in \mathbb{R}^{\mathcal{A} \times T}$.

Since affective features contain important information for perceiving emotions from gaits [15], we constrain a subset of the embeddings learned by our encoder to conform to these affective features. Specifically, we construct our embedding space to be $\mathbb{R}^{\mathcal{E} \times T}$ such that $\mathcal{E} \geq \mathcal{A}$. We then constrain the first $\mathcal{A} \times T$ dimensions of the embedding, denoted as $\hat{a}^{(i)}$ for the i^{th} gait, to be close to the corresponding gait affective features $a^{(i)}$. We term this the *affective loss* constraint, and express it as

$$\mathcal{L}_{\text{aff}} \left(a^{(i)}, \hat{a}^{(i)} \right) := \left\| a^{(i)} - \hat{a}^{(i)} \right\|^2. \quad (4)$$

The decoder for our autoencoder returns rotations per joint per time step as quaternions $(\hat{q}_j^t)^{(i)}$. Since quaternions for rotations have unit norm, we also use the following *quaternion loss* constraint,

$$\mathcal{L}_{\text{quat}} \left((\hat{q}_j^t)^{(i)} \right) := \left(\left\| (\hat{q}_j^t)^{(i)} \right\| - 1 \right)^2. \quad (5)$$

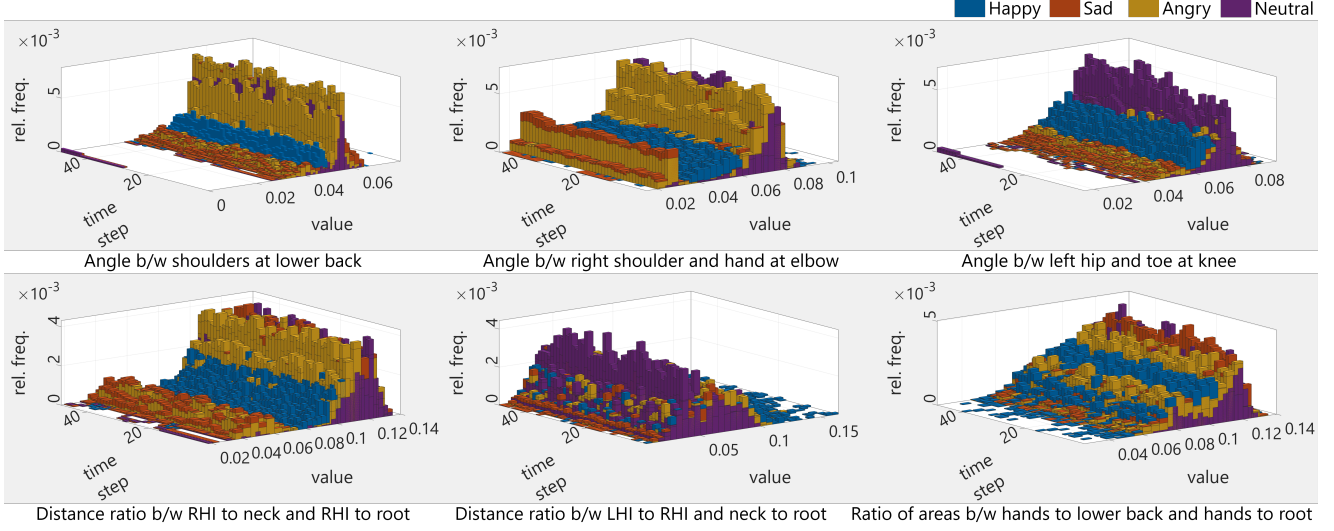


Figure 4. **Conditional distribution of affective features.** We show the distributions of 6 of the 18 affective features across all time steps, for the Emotion-Gait dataset, conditioned on the given class labels Happy, Sad, Angry, and Neutral. We observe that features for classes generally associated with more exaggerated joint movements, such as happy and angry, tend to overlap. We also observe that the features for these classes tend to be well-separated from features for sad and neutral classes, which are generally associated with more reserved joint movements.

Lastly, to measure the reconstruction loss for the autoencoder, we convert the input and the output quaternions to the corresponding Euler angles and compute the mean loss between the input and the output angles. We term this the *angle loss* and express it as

$$\mathcal{L}_{\text{ang}}(D^{(i)}, \hat{D}^{(i)}) := \left\| (D_X, D_Y, D_Z)^{(i)} - (\hat{D}_X, \hat{D}_Y, \hat{D}_Z)^{(i)} \right\|_F^2 \quad (6)$$

where $(D_X, D_Y, D_Z)^{(i)} \in [0, 2\pi]^{3J \times T}$ and $(\hat{D}_X, \hat{D}_Y, \hat{D}_Z)^{(i)} \in [0, 2\pi]^{3J \times T}$ denotes the set of Euler angles for all the joints across all the time steps for input $D^{(i)}$ and output $\hat{D}^{(i)}$, respectively, and $\|\cdot\|_F$ denotes the Frobenius norm.

Combining Eqs. 4, 5 and 6, we write the autoencoder loss $\mathcal{C}_{AE}(\cdot, \cdot)$ as

$$\mathcal{C}_{AE}(D^{(i)}, \hat{D}^{(i)}) := \mathcal{L}_{\text{ang}}(D^{(i)}, \hat{D}^{(i)}) + \lambda_{\text{quat}} \mathcal{L}_{\text{quat}} + \lambda_{\text{aff}} \mathcal{L}_{\text{aff}} \quad (7)$$

where λ_{quat} and λ_{aff} are the regularization parameters for the quaternion loss constraint and the affective loss constraint, respectively. In practice, to keep the scales of $\mathcal{L}_{\text{quat}}$ and \mathcal{L}_{aff} consistent, we scale all the affective features to lie in $[0, 1]$.

4. Network Architecture and Implementation

Our network for semi-supervised classification of discrete perceived emotions from gaits, shown in Figure 2, consists of three components, the encoder, the decoder, and

the classifier. We describe each of these components in turn and then summarize the training routine for our network.

4.1. Encoder

We first pass the sequences of gait motions on all the joints through a two-layer Gated Recurrent Unit (GRU). The GRU provides a feature representation for the rotation at each joint at each time step. We pass each of these representations through individual linear units. Following the kinematic chain of the human joints [5], we then pool the linear unit outputs for the two arms, the two legs, and the torso in five separate linear layers. In other words, each of these five linear layers learns to focus attention on a different part of the human body. The outputs from these five linear layers are then pooled into another linear layer, which, by construction, focuses attention on the motions of the entire body. For pooling, we perform vector addition as a way of composing the motions at the different hierarchies.

Our encoder thus learns the hierarchy of the joint motions in a bottom-up manner. The output of the last linear layer in the hierarchy is finally mapped to a feature representation in the embedding space of the encoder through another linear layer. In our case, the embedding space lies in $\mathbb{R}^{\mathcal{E} \times T}$ with $\mathcal{E} = 32$, which subsumes the space of affective features $\mathbb{R}^{\mathcal{A} \times T}$ with $\mathcal{A} = 18$, as discussed in Section 3.4.

4.2. Decoder

The decoder takes in the embedding from the encoder, repeats it five times for un-pooling, and passes the repeated

features through five linear layers. The outputs of these linear layers are features representing the reconstructed motions on the five parts, torso, two arms, and two legs. Each of these features is repeated for un-pooling, and then collectively fed into a GRU, which reconstructs the motion on every joint at a single step. A subsequent GRU takes in the reconstructed joint motions at a single time step and predicts the joint motions for the next $T - 1$ time steps.

4.3. Classifier

Our classifier takes in the embeddings and passes it through a series of 3 linear layers to generate the label probabilities. To make predictions, we set the output for a class to be 1 if the label probability for that class was more than $\frac{1}{C}$, similar to the routine for constructing input labels discussed in Section 3.3.

4.4. Training Routine

For training the network, we use the Adam optimizer [31] with a learning rate of 0.001, which we decay by a factor of 0.999 at every epoch. We use the ELU activation [14] on all the linear layers except the output layer, apply batch normalization [25] after every layer to reduce internal covariance-shift and apply a dropout of 0.1 to prevent overfitting during training. We also use the curriculum schedule [8] to speed up the training of the second GRU in the decoder. We begin training by presenting the input joint motions at every time step to the GRU, and the network predicts the joint motions at the subsequent time steps. This is equivalent to having a teacher forcing ratio of 1. At every epoch E , we decay the teacher forcing ratio by $\beta = 0.995$, *i.e.*, we provide the GRU the input joint motions with probability β^E or the GRU’s own predicted joint motions with probability $1 - \beta^E$ for it to predict the motions at the subsequent time steps. Curriculum scheduling helps the GRU to gently transition from a teacher-guided prediction routine to a self-guided prediction routine, which significantly speeds up the training process.

We train our network for 500 epochs, which takes around 4 hours on an Nvidia GeForce GTX 1080Ti GPU with 12 GB memory. We use 90% of the available labeled data and all the unlabeled data for training our network, and test its classification performance on the remaining 10% of the labeled data. We also observed that our network performs well for any values of λ_{quat} and λ_{aff} (in Eqn. 7) between 0.5 and 2.5. For the performance reported in our experiments in Section 5.3, we used a value of 2 for both.

5. Results

We perform experiments with the Emotion-Gait benchmark dataset [9]. It consists of 3D pose sequences of gaits collected from a variety of sources, for the purpose of emotion perception. We provide a brief description of

Table 2. **Average Precision scores.** Average precision (AP) per class and the mean average precision (mAP) over all the classes achieved by all the methods on the Emotion Gait dataset. Classes are Happy (H), Sad (S), Angry (A) and Neutral (N). Higher values are better. Bold indicates the best values of our method, blue indicates the best values from the methods we compare with.

Method	AP				mAP
	H	S	A	N	
STGCN [62]	0.98	0.83	0.42	0.18	0.61
DGNN [52]	0.99	0.90	0.76	0.37	0.76
LSTM Network [46]	0.96	0.84	0.62	0.51	0.73
STEP [9]	0.97	0.88	0.72	0.52	0.77
Our Method with only labeled data	0.98	0.86	0.71	0.51	0.77
Our Method w/o affective loss (AL)	0.96	0.88	0.70	0.59	0.78
Our Method with labeled data and AL	0.98	0.89	0.81	0.71	0.84

the dataset in Section 5.1. We list the methods we compare with in Section 5.2. We then summarize the results of the experiments we performed with this dataset on all these methods in Section 5.3.

5.1. Dataset

The Emotion-Gait dataset [9] consists of gaits collected from various 3D pose sequence datasets, including BML [35], Human3.6M [26], ICT [42], CMU-MoCap [1] and ELMD [21]. To maintain a uniform set of joints for the pose models collected from the different sources for training networks, all the models in Emotion-Gait were converted to the 21 joint pose model used in ELMD [21]. All input gaits are 240 frames long. We sample every 5th frame in the inputs and pass the resultant 48 frames as input data to our network, *i.e.*, $T = 48$ for all data points. In total, the dataset consists of 3,924 gaits of which 1,835 are annotated and remaining 2,089 are not annotated.

Histograms of Affective Features. We show histograms of the values of 6 of the 18 affective features we compute from the dataset in Figure 4. The histograms are plotted for all the 48 time steps in the input gaits and differently colored for inputs belonging to the different emotion classes as per the annotations. Inputs belonging to multiple classes are counted once in every class they belong to. We can observe from the histograms that for different affective features, different sets of classes have a high overlap of values while values of the other classes are well-separated. For example, there is a significant overlap in the values of the distance ratio between right hand index to neck and right hand index to root (Figure 4, bottom left) for gaits belonging to sad and angry classes, while the values of happy and neutral are distinct from these. Again, for gaits in happy and angry classes, there is a high overlap in the ratio of the area between hands to lower back and hands to root (Figure 4, bottom right), while the corresponding values for gaits in

neutral and sad classes are distinct from these.

The affective features also support observations in psychology corresponding to perceiving emotions from gaits. For example, slouching is generally considered to be an indicator of sadness [39]. Correspondingly, we can observe that the values of the angle between the shoulders at the lower back (Figure 4, top left) are lowest for sad gaits, indicating slouching.

5.2. Comparison Methods

We compare our method with state-of-the-art methods for both emotion recognition and action recognition from gaits. We choose to compare with action recognition methods since given a dataset of gaits, these methods only differ in the set of labels being learned. We list these methods below.

- **Emotion Recognition.** We compare with the method of Randhavane et al. [46], which combines affective features from gaits with features learned from an LSTM-based network taking pose sequences of gaits as input, to form hybrid feature vectors for classification. We also compare with STEP [9], which trains a spatial-temporal graph convolution-based network with gait inputs and affective features obtained from the gaits, and then fine-tunes the network with data generated from a graph convolution-based variational autoencoder.
- **Action Recognition.** We compare with recent state-of-the-art methods based on the spatial-temporal graph convolution network (STGCN) [62] and the directed graph neural network (DGNN) [52]. STGCN computes spatial neighborhoods as per the bone structure of the 3D poses and temporal neighborhoods according to the instances of the same joints across time steps and performs convolutions based on these neighborhoods to predict the output actions. DGNN computes directed acyclic graphs of the bone structure based on kinematic dependencies and trains a convolutional network with these graphs to learn action labels.

For a fair comparison, we retrained all these networks from scratch with the labeled portion of the Emotion-Gait dataset, following the reported training parameters, and a train test split of 9 : 1, same as that for our network.

Evaluation Metric. Since we deal with a multi-class, multi-label classification problem, we report the average precision (AP) achieved per class, which is computed as the mean of the precision values across all values of recall between 0 and 1. We also report the mean average precision, which is the mean of the average precisions (mAP) achieved in all the classes.

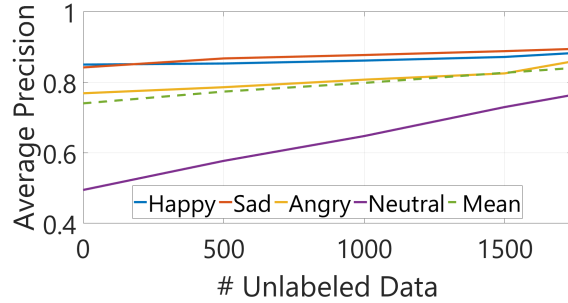


Figure 5. **AP increases with adding unlabeled data.** We observe that the average precision (AP) achieved on each class, as well as the mean AP over the classes, increases roughly linearly as we add more unlabeled data from the Emotion-Gait dataset to train our network. The increment is most significant for the neutral class, which has the fewest labels in the dataset. In practice, good techniques are available to extract (unlabeled) gaits from videos and thereby increase the accuracy of our approach.

5.3. Experiments

We summarize the AP and the mAP scores of all the methods in Table 2. Our method outperforms the next best-performing methods by around 7% on the absolute and outperforms the worst-performing method by 23% on the absolute.

Both the LSTM-based network and STEP consider per-frame affective features and inter-frame features such as velocities and rotations as inputs but do not explicitly model the dependencies between these two kinds of features. Our network, on the other hand, learns to embed a part of the features learned from joint rotations in the space of affective features. These embedded features, in turn, helps our network predict the output emotion labels with more precision.

The action recognition methods using STGCN and DGNN focus mostly on the movements of the leaf nodes in the poses, *i.e.*, hand indices, toes, and head. While these nodes are useful for distinguishing between motions such as walking and running, they do not contain sufficient information to distinguish between the various emotions.

Moreover, in the Emotion-Gait dataset, 58% of the data have happy labels, 32% have sad labels, 23% have angry labels and only 13% have neutral labels. Given this long-tail nature of the distribution, all the methods we compare with have more than 0.95 average precision in the happy and more than 0.80 average precision in the sad classes, but perform much poorer on the angry and the neutral classes. Our method, by contrast, learns to map the joint motions to the affective features, which helps it achieve around 10 – 50% better average precision on the absolute on the angry and the neutral class while maintaining similarly high average precision in the happy and the sad classes.

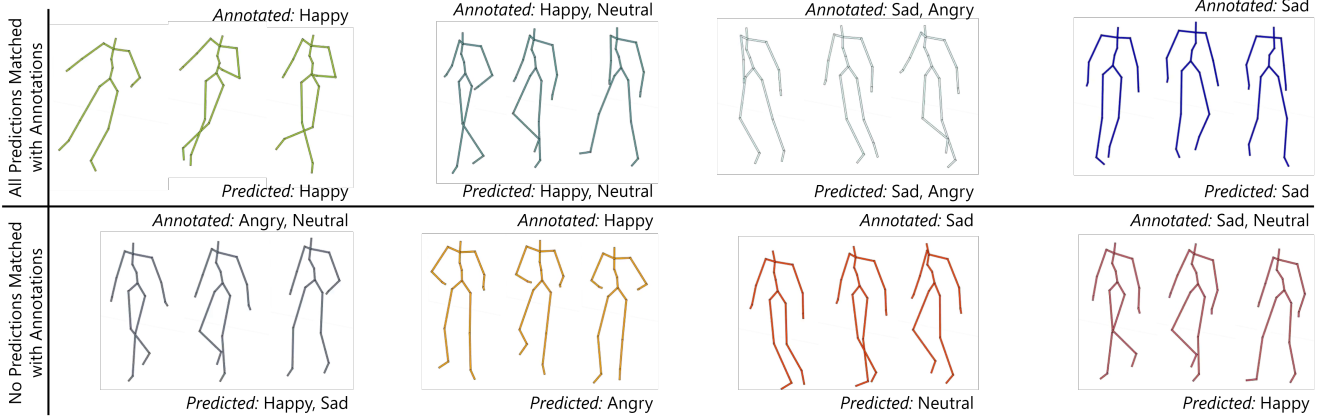


Figure 6. **Comparing predictions with annotations.** The top row shows 4 gaits from the Emotion-Gait dataset where the predicted labels of our network exactly matched the annotated input labels. The bottom row shows 4 gaits where the predicted labels did not match any of the input labels. Each gait is represented by 3 poses in temporal sequence from left to right. We observe that most of the disagreements are between either happy and angry or between sad and neutral, which is consistent with general observations in psychology.

Ablation Studies. We also perform ablation studies on our method to highlight the benefit of using both our semi-supervised approach as well as our affective loss constraint described in Eqn. 4.

First, we train our network only on the labeled dataset and obtain an mAP of 0.77, comparable to that of the next-best performing methods reported in Table 2.

Second, we remove the affective loss constraint from our loss function in Eqn. 7 and report the performance in Table 2. Without this constraint, the mean average precision drops by 6% on the absolute. More importantly, the average precisions on the angry and the neutral classes drop a significant 12% on the absolute, while the average precisions on the happy and the sad classes remain comparable. This highlights the benefit of using the affective loss constraints for learning the latent embeddings for all the classes, especially the ones with fewer labeled samples.

Adding Unlabeled Data: In practice, it is relatively easy to extract (unlabeled) gaits from video using pose extraction algorithms. We track the performance improvement of our network as we keep adding unlabeled data to our network. This result is summarized in Figure 5. We can observe that the mean average precision improves linearly as we keep adding more data. The trend does not indicate a saturation in performance even after adding all the 2,089 unlabeled data. This suggests that the performance of our approach can increase with more unlabeled gait data.

5.4. Qualitative Results

We show the qualitative results of our network in Figure 6. The top row in the Figure shows cases where the predicted labels for a gait exactly matched all the corresponding annotated labels. We observe that the gaits with happy

and angry labels in the annotation have more animated joint movements compared to the gaits with sad and neutral labels, which our network was able to successfully learn from the affective features.

The bottom row in the Figure shows cases where the predicted labels for a gait did not match any of the annotated labels. We notice that most disagreements arise either between sad and neutral labels or between happy and angry labels. This again follows the observation that both happy and angry gaits often have more exaggerated joint movements, while both sad and neutral gaits often have more reserved joint movements. There are also disagreements between happy and neutral labels for some gaits, which we associate with the subjectivity in emotion perception.

6. Limitations and Future Work

Our work has some limitations. Firstly, we consider only discrete emotions of people and do not map these to the underlying continuous emotion space given by the VAD model [38]. Even though discrete emotions are presumably easier to work with for non-expert end-users, we plan to extend our method to work in the continuous space of emotions, *i.e.*, given a gait, our network regresses it to a point in the VAD space that indicates the perceived emotions.

Second, our network only looks at low-level features of gaits to predict perceived emotions. In the future, we plan to add higher-level information, such as the presence of other people in the vicinity, background context, etc. that are known to influence a person’s emotions [33, 34], to further sophisticate the performance of our network.

References

- [1] Cmu graphics lab motion capture database. <http://mocap.cs.cmu.edu/>, 2018.
- [2] Unaiza Ahsan, Chen Sun, and Irfan Essa. Discrim-net: Semi-supervised action recognition from videos using generative adversarial networks. *arXiv preprint arXiv:1801.07230*, 2018.
- [3] J Arunnehr and M Kalaiselvi Geetha. Automatic human emotion recognition in surveillance video. In *IT-SPMS*, pages 321–342. Springer, 2017.
- [4] Ashwin Ramesh Babu, Akilesh Rajavenkatanarayanan, James Robert Brady, and Fillia Makedon. Multimodal approach for cognitive task performance prediction from body postures, facial expressions and eeg signal. In *Proceedings of the Workshop on Modeling Cognitive Processes from Multimodal Data*, page 2. ACM, 2018.
- [5] Norman I Badler, Cary B Phillips, and Bonnie Lynn Webber. *Simulating humans: computer graphics animation and control*. Oxford University Press, 1993.
- [6] Lisa Feldman Barrett. *How emotions are made: The secret life of the brain*. Houghton Mifflin Harcourt, 2017.
- [7] Andrea Bauer et al. The autonomous city explorer: Towards natural human-robot interaction in urban environments. *IJSR*, 1(2):127–140, 2009.
- [8] Samy Bengio, Oriol Vinyals, Navdeep Jaitly, and Noam Shazeer. Scheduled sampling for sequence prediction with recurrent neural networks. In *Advances in Neural Information Processing Systems*, pages 1171–1179, 2015.
- [9] Uttaran Bhattacharya, Trisha Mittal, Rohan Chandra, Tanmay Randhavane, Aniket Bera, and Dinesh Manocha. Step: Spatial temporal graph convolutional networks for emotion perception from gaits. *arXiv preprint arXiv:1910.12906*, 2019.
- [10] Haoye Cai, Chunyan Bai, Yu-Wing Tai, and Chi-Keung Tang. Deep video generation, prediction and completion of human action sequences. In *ECCV*, pages 366–382, 2018.
- [11] Joao Carreira and Andrew Zisserman. Quo vadis, action recognition? a new model and the kinetics dataset. In *proceedings of the IEEE Conference on Computer Vision and Pattern Recognition*, pages 6299–6308, 2017.
- [12] Ying Chen, Wenjun Hou, Xiyao Cheng, and Shoushan Li. Joint learning for emotion classification and emotion cause detection. In *Proceedings of the 2018 Conference on Empirical Methods in Natural Language Processing*, pages 646–651, 2018.
- [13] Vasileios Choutas, Philippe Weinzaepfel, Jérôme Revaud, and Cordelia Schmid. Potion: Pose motion representation for action recognition. In *Proceedings of the IEEE Conference on Computer Vision and Pattern Recognition*, pages 7024–7033, 2018.
- [14] Djork-Arné Clevert, Thomas Unterthiner, and Sepp Hochreiter. Fast and accurate deep network learning by exponential linear units (elus). *arXiv preprint arXiv:1511.07289*, 2015.
- [15] Arthur Crenn, Rizwan Ahmed Khan, Alexandre Meyer, and Saida Bouakaz. Body expression recognition from animated 3d skeleton. In *IC3D*, pages 1–7. IEEE, 2016.
- [16] Mohamed Daoudi, Stefano Berretti, Pietro Pala, Yvonne Delevoye, and Alberto Del Bimbo. Emotion recognition by body movement representation on the manifold of symmetric positive definite matrices. In *ICIAP*, pages 550–560. Springer, 2017.
- [17] P Ekman and W V Friesen. Head and body cues in the judgment of emotion: A reformulation. *Perceptual and motor skills*, 1967.
- [18] C. Fabian Benitez-Quiroz, Ramprakash Srinivasan, and Aleix M. Martinez. Emotionet: An accurate, real-time algorithm for the automatic annotation of a million facial expressions in the wild. In *CVPR*, June 2016.
- [19] José-Miguel Fernández-Dols and Maria-Angeles Ruiz-Belda. Expression of emotion versus expressions of emotions. In *Everyday conceptions of emotion*, pages 505–522. Springer, 1995.
- [20] F Sebastian Grassia. Practical parameterization of rotations using the exponential map. *Journal of graphics tools*, 3(3):29–48, 1998.
- [21] Ikhansul Habibie, Daniel Holden, Jonathan Schwarz, Joe Yearsley, and Taku Komura. A recurrent variational autoencoder for human motion synthesis. In *Proceedings of the British Machine Vision Conference (BMVC)*, 2017.
- [22] Félix G Harvey, Julien Roy, David Kanaa, and Christopher Pal. Recurrent semi-supervised classification and constrained adversarial generation with motion capture data. *Image and Vision Computing*, 78:42–52, 2018.
- [23] Holger Hoffmann, Andreas Scheck, Timo Schuster, Steffen Walter, Kerstin Limbrecht, Harald C Traue, and Henrik Kessler. Mapping discrete emotions into the dimensional space: An empirical approach. In *2012 IEEE International Conference on Systems, Man, and Cybernetics (SMC)*, pages 3316–3320. IEEE, 2012.

- [24] Daniel Holden, Jun Saito, and Taku Komura. A deep learning framework for character motion synthesis and editing. *ACM Transactions on Graphics (TOG)*, 35(4):138, 2016.
- [25] Sergey Ioffe and Christian Szegedy. Batch normalization: Accelerating deep network training by reducing internal covariate shift. *arXiv preprint arXiv:1502.03167*, 2015.
- [26] Catalin Ionescu, Dragos Papava, Vlad Olaru, and Cristian Sminchisescu. Human3.6m: Large scale datasets and predictive methods for 3d human sensing in natural environments. *IEEE transactions on pattern analysis and machine intelligence*, 36(7):1325–1339, 2013.
- [27] Agnes Jacob and P Mythili. Prosodic feature based speech emotion recognition at segmental and supra segmental levels. In *SPICES*, pages 1–5. IEEE, 2015.
- [28] Angjoo Kanazawa, Jason Y Zhang, Panna Felsen, and Jitendra Malik. Learning 3d human dynamics from video. In *Proceedings of the IEEE Conference on Computer Vision and Pattern Recognition*, pages 5614–5623, 2019.
- [29] Michelle Karg, Kolja Kuhnlenz, and Martin Buss. Recognition of affect based on gait patterns. *Cybernetics*, 40(4):1050–1061, 2010.
- [30] Mehran Khodabandeh, Hamid Reza Vaezi Joze, Ilya Zharkov, and Vivek Pradeep. Diy human action dataset generation. In *Proceedings of the IEEE Conference on Computer Vision and Pattern Recognition Workshops*, pages 1448–1458, 2018.
- [31] Diederik P Kingma and Jimmy Ba. Adam: A method for stochastic optimization. *arXiv preprint arXiv:1412.6980*, 2014.
- [32] Andrea Kleinsmith and Nadia Bianchi-Berthouze. Affective body expression perception and recognition: A survey. *IEEE Transactions on Affective Computing*, 4(1):15–33, 2013.
- [33] Ronak Kosti, Jose Alvarez, Adria Recasens, and Agata Lapedriza. Context based emotion recognition using emotic dataset. *IEEE transactions on pattern analysis and machine intelligence*, 2019.
- [34] Jiyoung Lee, Seungryong Kim, Sunok Kim, Jungin Park, and Kwanghoon Sohn. Context-aware emotion recognition networks. *arXiv preprint arXiv:1908.05913*, 2019.
- [35] Yingliang Ma, Helena M Paterson, and Frank E Pollick. A motion capture library for the study of identity, gender, and emotion perception from biological motion. *Behavior research methods*, 38(1):134–141, 2006.
- [36] Hanneke KM Meeren, Corné CRJ van Heijnsbergen, and Beatrice de Gelder. Rapid perceptual integration of facial expression and emotional body language. *Proceedings of NAS*, 102(45):16518–16523, 2005.
- [37] Albert Mehrabian. Analysis of the big-five personality factors in terms of the pad temperament model. *Australian journal of Psychology*, 48(2):86–92, 1996.
- [38] Albert Mehrabian and James A Russell. *An approach to environmental psychology*. the MIT Press, 1974.
- [39] Johannes Michalak, Nikolaus F Troje, Julia Fischer, Patrick Vollmar, Thomas Heidenreich, and Dietmar Schulte. Embodiment of sadness and depression gait patterns associated with dysphoric mood. *Psychosomatic Medicine*, 71(5):580–587, 2009.
- [40] J Mikels, B Fredrickson, et al. Emotional category data on images from the international affective picture system. *Behavior research methods*, 2005.
- [41] Joann M Montepare, Sabra B Goldstein, and Annmarie Clausen. The identification of emotions from gait information. *Journal of Nonverbal Behavior*, 11(1):33–42, 1987.
- [42] Sahil Narang, Andrew Best, Andrew Feng, Sin-hwa Kang, Dinesh Manocha, and Ari Shapiro. Motion recognition of self and others on realistic 3d avatars. *Computer Animation and Virtual Worlds*, 28(3-4):e1762, 2017.
- [43] Richard E Nisbett and Timothy D Wilson. Telling more than we can know: Verbal reports on mental processes. *Psychological review*, 84(3):231, 1977.
- [44] Dario Pavllo, Christoph Feichtenhofer, David Grangier, and Michael Auli. 3d human pose estimation in video with temporal convolutions and semi-supervised training. In *Proceedings of the IEEE Conference on Computer Vision and Pattern Recognition*, pages 7753–7762, 2019.
- [45] Dario Pavllo, David Grangier, and Michael Auli. Quaternet: A quaternion-based recurrent model for human motion. *arXiv preprint arXiv:1805.06485*, 2018.
- [46] Tanmay Randhavane, Aniket Bera, Kyra Kapskakis, Uttaran Bhattacharya, Kurt Gray, and Dinesh Manocha. Identifying emotions from walking using affective and deep features. *arXiv preprint arXiv:1906.11884*, 2019.
- [47] K. Sreenivasa Rao, Shashidhar G. Koolagudi, and Ramu Reddy Vempada. Emotion recognition from speech using global and local prosodic features. *International Journal of Speech Technology*, 2013.
- [48] Heidi R. Riggio. Emotional expressiveness. *Encyclopedia of Personality and Individual Differences*, 2017.

- [49] Jesús J Rivas, Felipe Orihuela-Espina, L Enrique Su-car, Lorena Palafox, Jorge Hernández-Franco, and Na-dia Bianchi-Berthouze. Detecting affective states in virtual rehabilitation. In *Proceedings of the 9th International Conference on Pervasive Computing Technologies for Healthcare*, pages 287–292. ICST (Institute for Computer Sciences, Social-Informatics and , 2015.
- [50] MW Schurgin, J Nelson, S Iida, H Ohira, JY Chiao, and SL Franconeri. Eye movements during emotion recognition in faces. *Journal of vision*, 14(13):14–14, 2014.
- [51] Amir Shahroudy, Jun Liu, Tian-Tsong Ng, and Gang Wang. Ntu rgb+ d: A large scale dataset for 3d human activity analysis. In *Proceedings of the IEEE conference on computer vision and pattern recognition*, pages 1010–1019, 2016.
- [52] Lei Shi, Yifan Zhang, Jian Cheng, and Hanqing Lu. Skeleton-based action recognition with directed graph neural networks. In *Proceedings of the IEEE Conference on Computer Vision and Pattern Recognition*, pages 7912–7921, 2019.
- [53] Lei Shi, Yifan Zhang, Jian Cheng, and Hanqing Lu. Two-stream adaptive graph convolutional networks for skeleton-based action recognition. In *Proceedings of the IEEE Conference on Computer Vision and Pattern Recognition*, pages 12026–12035, 2019.
- [54] Chenyang Si, Wentao Chen, Wei Wang, Liang Wang, and Tieniu Tan. An attention enhanced graph convolutional lstm network for skeleton-based action recognition. In *Proceedings of the IEEE Conference on Computer Vision and Pattern Recognition*, pages 1227–1236, 2019.
- [55] Sebastian Starke, He Zhang, Taku Komura, and Jun Saito. Neural state machine for character-scene interactions. *ACM Transactions on Graphics*, 38(6), 7 2019.
- [56] Carlo Strapparava and Rada Mihalcea. Learning to identify emotions in text. In *Proceedings of the 2008 ACM symposium on Applied computing*, pages 1556–1560. ACM, 2008.
- [57] Gentiane Venture, Hideki Kadone, Tianxiang Zhang, Julie Grèzes, Alain Berthoz, and Halim Hicheur. Recognizing emotions conveyed by human gait. *IJSR*, 6(4):621–632, 2014.
- [58] Lei Wang, Du Q Huynh, and Piotr Koniusz. A comparative review of recent kinect-based action recognition algorithms. *arXiv preprint arXiv:1906.09955*, 2019.
- [59] Zuxuan Wu, Yanwei Fu, Yu-Gang Jiang, and Leonid Sigal. Harnessing object and scene semantics for large-scale video understanding. In *Proceedings of the IEEE Conference on Computer Vision and Pattern Recognition*, pages 3112–3121, 2016.
- [60] An Yan, Yali Wang, Zhifeng Li, and Yu Qiao. Pa3d: Pose-action 3d machine for video recognition. In *Proceedings of the IEEE Conference on Computer Vision and Pattern Recognition*, pages 7922–7931, 2019.
- [61] Sijie Yan, Zhizhong Li, Yuanjun Xiong, Huahan Yan, and Dahua Lin. Convolutional sequence generation for skeleton-based action synthesis. In *Proceedings of the IEEE International Conference on Computer Vision*, pages 4394–4402, 2019.
- [62] Sijie Yan, Yuanjun Xiong, and Dahua Lin. Spatial temporal graph convolutional networks for skeleton-based action recognition. In *AAAI*, 2018.
- [63] Ceyuan Yang, Zhe Wang, Xinge Zhu, Chen Huang, Jianping Shi, and Dahua Lin. Pose guided human video generation. In *Proceedings of the European Conference on Computer Vision (ECCV)*, pages 201–216, 2018.
- [64] Ceyuan Yang, Zhe Wang, Xinge Zhu, Chen Huang, Jianping Shi, and Dahua Lin. Pose guided human video generation. In *ECCV*, pages 201–216, 2018.
- [65] Jason Y Zhang, Panna Felsen, Angjoo Kanazawa, and Jitendra Malik. Predicting 3d human dynamics from video. In *Proceedings of the IEEE International Conference on Computer Vision*, pages 7114–7123, 2019.
- [66] Songyang Zhang, Yang Yang, Jun Xiao, Xiaoming Liu, Yi Yang, Di Xie, and Yueting Zhuang. Fusing geometric features for skeleton-based action recognition using multilayer lstm networks. *IEEE Transactions on Multimedia*, 20(9):2330–2343, 2018.